NJC

PAPER

View Article Online
View Journal | View Issue

Cite this: *New J. Chem.*, 2016, **40**, 1655

Effect of fluorination pattern and extent on the properties of PCDTBT derivatives†

Luke Cartwright, Hunan Yi and Ahmed Iraqi*

Received (in Montpellier, France) 7th September 2015,
Accepted 8th December 2015

DOI: 10.1039/c5nj02394g

www.rsc.org/njc

Herein, we report the synthesis of a series of fluorinated dithienyl carbazole-*alt*-benzothiadiazoles (**PCDTBT** analogues) and the characterisation of their optical, electrochemical, thermal and molecular organisation in the solid state. The polymers were decorated with fluorine on either the benzothiadiazole unit, carbazole unit or both to yield **PCDTffBT**, **PCffDTBT** and **PCffDTffBT**, respectively. The copolymers displayed decomposition temperatures in excess of 350 °C. **PCDTffBT**, **PCffDTBT** and **PCffDTffBT** displayed optical band gaps of 1.86, 1.82 and 1.88 eV, respectively. It was speculated this was a consequence of the higher molecular weight of **PCffDTBT** relative to the other polymers. **PCffDTBT** and **PCffDTffBT** displayed shallower HOMO levels relative to **PCDTffBT**; a consequence of fluorinating the carbazole-donor moiety. XRD studies confirmed that fluorinating the benzothiadiazole-acceptor moiety improves molecular ordering by promoting π–π stacking of polymer backbones in solid state. Interestingly, fluorinating the carbazole-donor unit does not improve π–π stacking of polymer backbones.

Introduction

Carbazole, is an appealing building-block for the development of conjugated copolymers.[1] Carbazole is structurally analogous to fluorene, which has also found widespread use in optoelectronic devices. However, the presence of an electron-donating nitrogen atom in its central fused pyrrole ring renders carbazole fully aromatic, unlike fluorene.[1] Replacing the 9*H*-carbon with nitrogen in the fluorene skeleton bestows further desirable properties upon the resulting unit including: (1) increased oxidative stability owing to the propensity for the 9*H*-position of fluorene to undergo oxidation to the ketone product, which results in adverse physical properties.[2] (2) The nitrogen in the central pyrrole ring can be functionalised to improve the physical properties of the resulting polymer.[3–5] Consequently, carbazole-based conjugated polymers are easy to synthesise, display excellent photochemical and thermal stabilities and possess high charge carrier mobilities.[1] Thus, carbazole-based conjugated polymers and their derivatives have found extensive use in organic light emitting diodes (OLEDs), organic thermal electronic devices, organic field-effect transistors (OFETs) and organic photovoltaics (OPV).[6–11]

It could be argued that poly[*N*-9′-heptadecanyl-2,7-carbazole-*alt*-5,5-(4′,7′-di-2-thienyl-2′,1′,3′-benzothiadiazole)] (**PCDTBT**) and its derivatives are the most studied carbazole-based donor–acceptor (D–π–A) conjugated polymers. **PCDTBT** has found widespread use in organic photovoltaic (OPV) devices and efficiencies in excess of 7% have been achieved when blended with the fullerene derivative $PC_{70}BM$.[10] This is by no means the highest efficiency recorded in OPV devices.[12–14] However, the thermal and oxidative stability, deep HOMO level and ease of processability have allowed **PCDTBT** to remain an attractive conjugated polymer for optoelectronic applications.[15,16]

The body of literature concerning the incorporation of fluorine as a substituent and the effect it has on the resulting polymer system is expanding rapidly.[17–20] However, fluorination of **PCDTBT** has received little attention, which is surprising considering the promise **PCDTBT** and its derivatives have displayed in optoelectronic devices.[21–24] Imahori and co-workers investigated the effects of fluorine substitution on **PCDTBT** by copolymerising a fluorinated benzothiadiazole-acceptor with a carbazole-donor to yield **PCDTBT-F**.[24] The introduction of two fluorine atoms on the 5,6-positions of benzothiadiazole decreased the HOMO energy level of **PCDTBT-F**, relative to that of **PCDTBT**. However, **PCDTBT-F** displayed a significantly reduced molecular weight, poor solubility, blue-shifted absorption maxima and a larger optical band-gap, relative to **PCDTBT**.[24] In contrast, Bo *et al.* reported the polymerisation of a fluorinated-carbazole donor with a dialkoxy-substituted benzothiadiazole acceptor to yield **PDFCDTBT**.[21] The introduction of fluorine atoms at the 3,6-positions of carbazole yielded a moderate molecular weight polymer with deeper frontier energy levels, red-shifted absorption maxima and a smaller

Department of Chemistry, University of Sheffield, Sheffield, S3 7HF, UK.
E-mail: a.iraqi@sheffield.ac.uk.ac.uk; Fax: +44 (0)114 222 9303;
Tel: +44 (0)114 222 9566

† Electronic supplementary information (ESI) available: ^{1}H-NMR spectra of the final monomers and the polymers. See DOI: 10.1039/c5nj02394g

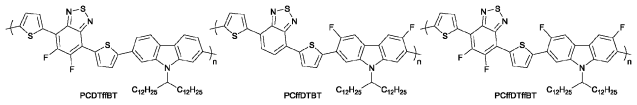

Fig. 1 Structures of **PCDTffBT**, **PCffDTBT** and **PCffDTffBT**.

optical band gap, relative to its non-fluorinated counterpart. Furthermore, **PDFCDTBT** displayed more organised packing in solid state.[21]

With this is mind, we report the synthesis of three fluorinated carbazole-*alt*-benzothiadiazole conjugated polymers. Fluorine was attached to either the benzothiadiazole unit, carbazole unit or both units to yield **PCDTffBT**, **PCffDTBT** and **PCffDTffBT**, respectively (Fig. 1). Imahori reported that the fluorinated **PCDTBT** analogue they synthesised forms a low molecular weight polymer with poor solubility. Thus, the polymers in this work were designed to bear larger solubilising chains on the carbazole moiety in the hope that higher molecular weight polymers could be obtained. The optical, electrochemical, thermal and structural properties of the polymers in the solid state are probed in order to ascertain the effects fluorination has on the resulting polymer.

Results and discussion

Polymer synthesis

The synthetic route for the preparation of 2,7-dibromo-3,6-difluoro-9-(pentacosan-13-yl)-9*H*-carbazole (**M1**) is outlined in Scheme 1. **M1** was synthesised starting from the commercially available 1,4-dibromo-2-fluorobenzene. 2,7-Dibromo-9-(pentacosan-13-yl)-9*H*-carbazole (**M2**) was synthesised according to a modified literature procedure.[25] 4,7-Bis(5-(trimethylstannyl)thiophene-2-yl)benzo[*c*][1,2,5]thiadiazole (**M3**) and 5,6-difluoro-4,7-bis(5-(trimethylstannyl)thiophene-2-yl)benzo[*c*][1,2,5]thiadiazole (**M4**) were synthesised from 4,7-di(thiophen-2-yl)benzo[*c*][1,2,5]thiadiazole and 5,6-difluoro-4,7-di(thiophene-2-yl)benzo[*c*][1,2,5]thiadiazole, respectively. Deprotonation of the starting material with lithium 2,2,6,6-tetramethylpiperidine (LTMP) and subsequent treatment with trimethyltin chloride afforded **M3** and **M4** (Scheme 1). Stille polycondensation of **M2** with **M4**, **M1** with **M3** and **M1** with **M4** yielded **PCDTffBT**, **PCffDTBT** and **PCffDTffBT**, respectively (Scheme 1). $Pd(OAc)_2$ and tri(*o*-tolyl)phosphine ($P(o\text{-tol})_3$) were used as the catalyst and toluene as the solvent. All polymerisations were left for 48 hours. The polymers were cleaned *via* Soxhlet extraction using in turn methanol, acetone, hexane and toluene. The toluene fractions were collected, reduced *in vacuo* and precipitated in methanol. Subsequent studies were conducted on the toluene fractions only. ^{1}H-NMR and elemental analysis were used to verify the structure of **PCDTffBT**, **PCffDTBT** and **PCffDTffBT**. Gel permeation chromatography (GPC) using 1,2,4-trichlorobenzene as the eluent, at 140 °C was used to determine the number-average molecular weight (M_n) and weight-average molecular weight (M_w) of the polymers synthesised. **PCffDTBT** displayed the highest M_n and M_w of all polymers synthesised with values of 11 400 and 20 600 Da, respectively. Both **PCDTffBT** and **PCffDTffBT** displayed significantly reduced molecular weights relative to **PCffDTBT** with values of 11 900 and 8900 Da, respectively (Table 1). Previous literature has speculated that fluorination of the benzothiadiazole unit moiety promotes π–π stacking and aggregation of polymer chains, which impedes the solubility of the polymer and its attainable molecular weight.[26] The results obtained here support this hypothesis.

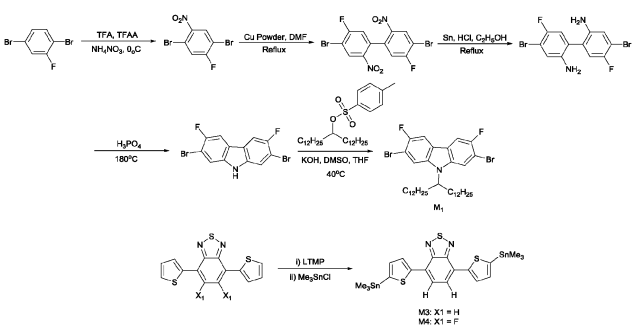

Scheme 1 Synthetic routes to the final monomer products: **M1**, **M3** and **M4**. **M2** was synthesised using previously established literature procedures.

PCDTBT-F synthesised by Imahori and co-workers is an analogous polymer to **PCDTffBT**.[24] **PCDTBT-F** has C17-branched substituents rather than C25-branched substituents for **PCDTffBT**. It was reported that **PCDTBT-F** displayed poor solubility which limited the molecular weight of the resulting polymer (M_w = 6000 Da). Thus, **PCDTffBT** was designed to bear larger solubilising chains on the carbazole moiety in the hope that a higher molecular weight polymer could be obtained. **PCDTffBT** does possess a higher M_w (11 900 Da), relative to **PCDTBT-F**. **PCffDTffBT** in which both the carbazole and benzothiadiazole repeat units have fluorine substituents, has the most reduced processability in this series of polymers. Both the yield of the soluble toluene fraction and the molecular weight of this polymer are lower compared to the other two polymers presented in this work.

Optical properties

The optical properties of all polymers were investigated by UV-vis absorption spectroscopy on dilute chloroform solutions and drop-cast films on quartz substrates (Fig. 2). The optical properties of the polymers are summarised in Table 1. All polymers exhibit two absorption peaks in both solution and film states. The absorption band at shorter wavelengths can be ascribed to the π–π* transition. In contrast, the absorption band at longer wavelengths can be attributed to intramolecular charge transfer between the dithienyl-carbazole donor moieties and the benzothiadiazole acceptor units. All polymers undergo a bathochromic shift when cast into a thin-film, relative to their solution absorption. This can be ascribed to stronger π–π interchain stacking and a more coplanar structure in solid state. The λ_{max} of **PCDTffBT**, **PCffDTBT** and **PCffDTffBT** are located at 556, 558 and 545 nm in film states. The optical band gaps of **PCDTffBT**, **PCffDTBT** and **PCffDTffBT**, as determined from the onset of absorption, were estimated to be 1.86, 1.82 and 1.88 eV, respectively. Furthermore, **PCffDTffBT** displayed improved resolution in the solid-state with the presence

Table 1 A summary of the GPC, UV-vis absorption and fluorescence data for **PCDTffBT**, **PCffDTBT** and **PCffDTffBT**

				UV-vis absorption				Fluorescence		
Polymer	M_n [a]	M_w [a]	PDI	λ_{max} solution (nm)	ε [b] (M^{-1} cm^{-1})	λ_{max} film (nm)	E_g^{opt} film [c] (eV)	λ_{max} solution (nm)	λ_{max} film (nm)	Stokes shift [d] (nm)
PCDTffBT	7700	11 900	1.55	379, 526	49 900	395, 556	1.86	618	710	154
PCffDTBT	11 400	20 600	1.81	381, 526	40 600	404, 558	1.82	637	712	154
PCffDTffBT	6100	8900	1.46	387, 520	43 000	401, 545	1.88	600	712	167

[a] Measurements conducted on the toluene fraction of the polymer using differential refractive index (DRI) detection. [b] Absorption coefficient measured at λ_{max} in chloroform solution. [c] Optical energy gap determined from the onset of the absorption band in thin film. [d] Stokes shift determined from film studies.

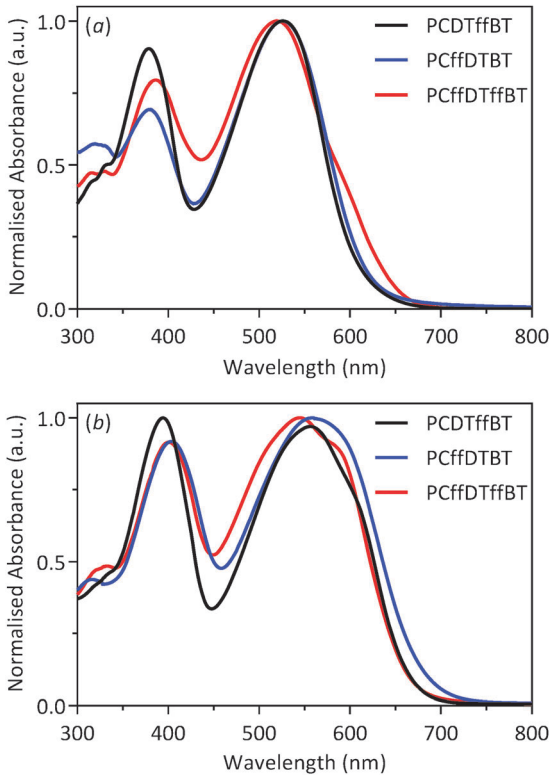

Fig. 2 Normalised UV-vis absorption spectra of **PCDTffBT**, **PCffDTBT** and **PCffDTffBT** in: (a) chloroform solution; and (b) thin films.

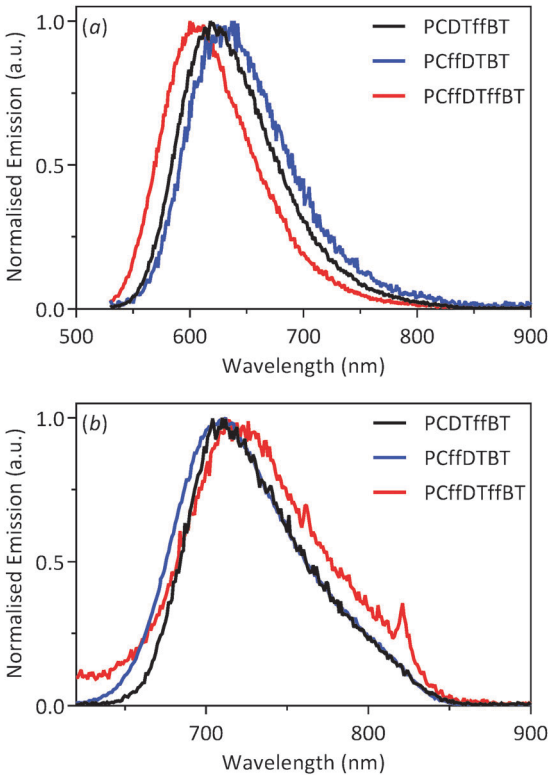

Fig. 3 Normalised fluorescence spectra of **PCDTffBT**, **PCffDTBT** and **PCffDTffBT** in: (a) chloroform solution; and (b) thin films.

of shoulder peak at ~580 nm, which we attribute to a higher tendency of aggregation of polymer chains for this polymer compared to the other two polymers in the series; a consequence of improved molecular arrangement in solid state. The higher M_w of **PCffDTBT** did not translate into significantly higher λ_{max} value. However, the optical band gap of **PCffDTBT** was lower than **PCDTffBT** and **PCffDTffBT**. It would appear that in this series of polymers, fluorination of the carbazole moiety affords a polymer with the lowest optical band gap allowing the resulting polymer to harvest a larger portion of the solar spectrum. It is also worth noting that the optical band gap of non-fluorinated **PCDTBT** (1.88 eV)[11] is similar to those of **PCDTffBT** and **PCffDTffBT**.

The fluorescence spectra of the polymers in solution and solid films are illustrated in Fig. 3. All fluorescence spectra were recorded upon exciting the polymers at their absorption maxima. In solution **PCDTffBT**, **PCffDTBT** and **PCffDTffBT** exhibited emission maxima at 618, 637 and 600 nm, respectively. The emission maxima are red-shifted to 710, 712 and 712 nm for **PCDTffBT**, **PCffDTBT** and **PCffDTffBT**, respectively. It is suspected that the large difference in the solution emission maxima is due to interactions between the local solvent environment and the fluorophore. Solvent molecules stabilise and lower the energy of the excited state of **PCffDTBT**; resulting in a red-shift in the solution fluorescence emission. Once the polymers have been cast into films, the effects of solvent relaxation no longer apply, and the polymers exhibit a fluorescence emission at similar wavelengths. The large Stokes shifts of 154, 154 and 167 nm for **PCDTffBT**, **PCffDTBT** and **PCffDTffBT**, respectively, suggests there is a significant energy difference between the ground state and excited state of the polymers.

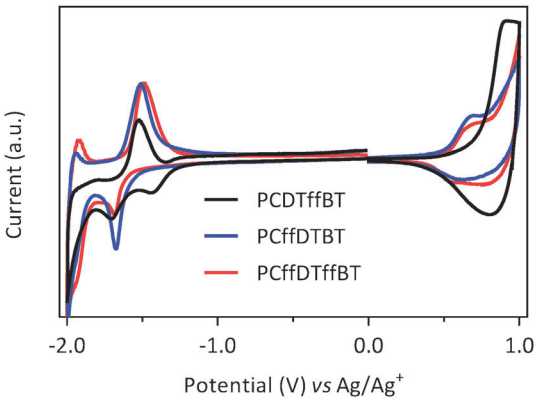

Fig. 4 Cyclic voltammograms of **PCDTffBT**, **PCffDTBT** and **PCffDTffBT** on platinum disc electrodes (area 0.031 cm^2) at a scan rate of 100 mV s^{-1} in acetonitrile/tetrabutyl ammonium perchlorate (0.1 mol dm^{-3}).

Electrochemical properties

Cyclic voltammetry was used to determine the HOMO and LUMO energy levels (*vs.* vacuum) of drop-cast polymer films in acetonitrile with tetrabutylammonium perchlorate as the electrolyte (Fig. 4 and Table 2). **PCDTffBT** displayed the deepest HOMO level of all polymers synthesised with a value of −5.44 eV, which is deeper than its non-fluorinated analogue, **PCDTBT**.[11] The LUMO level of **PCDTffBT** was measured to be −3.45 eV, which is slightly lower than **PCDTBT**.[11] This is consistent with previous literature concerning the effects of fluorine substitution and the effects it has the resulting polymers HOMO levels.[27–31]

The HOMO level of **PCffDTBT** was calculated to be −5.23 eV. This is similar to the HOMO of level of **PDFCDTBT** reported by Bo and co-workers.[21] However, it is significantly shallower than **PCDTBT**.[11] The electrochemistry results suggest that fluorination of the carbazole-moiety results in it becoming a significantly stronger donor unit. Generally, fluorine is considered to be a deactivating substituent, thus, this result may seem erroneous. However, it is known that fluorine as a substituent on an aromatic benzene is considered to be both σ-electron withdrawing and π-electron donating.[32] The π-donating ability of fluorine is reflected in the anomalously high *para*-position reactivity.[33] Fluorobenzene displays a higher proton affinity than benzene, another example of the anomalously high reactivity of fluorobenzene relative to benzene.[34,35] We speculate that fluorination of the carbazole moiety increases the π-electron density of the resulting monomer unit. Consequently, the fluorinated carbazole moiety is a stronger donor resulting in a shallower HOMO level. It is possible that this will negatively impact the oxidative stability of the **PCffDTBT**.

Table 2 A summary of the TGA and electrochemical data for **PCDTffBT**, **PCffDTBT** and **PCffDTffBT**

Polymer	T_d [a] (°C)	HOMO[b] (eV)	LUMO[c] (eV)	E_g^{elec} [d] (eV)
PCDTffBT	367	−5.44	−3.45	1.99
PCffDTBT	390	−5.23	−3.12	2.11
PCffDTffBT	351	−5.24	−3.11	2.13

[a] Onset of degradation as determined *via* thermogravimetric analysis (TGA) with a heating rate of 10 °C min^{-1} under an inert atmosphere of nitrogen. [b] HOMO position (*vs.* vacuum) determined from the onset of oxidation. [c] LUMO position (*vs.* vacuum) determined from the onset of reduction. [d] Electrochemical energy gap.

Thermal properties

Thermogravimetric analysis of **PCDTffBT**, **PCffDTBT** and **PCffDTffBT** revealed that all polymers possess good thermal stability with degradation temperatures in excess of 350 °C (Fig. 5). The onset of degradation (5% weight loss) for **PCDTffBT**, **PCffDTBT** and **PCffDTffBT** were estimated to be 367, 390 and 351 °C (Table 2). We tentatively speculate that the degradation temperature of these polymers is dependent upon the molecular weight. We hypothesise that the lower molecular weights of **PCDTffBT** and **PCffDTffBT** have two effects on the polymer properties. Firstly, **PCDTffBT** and **PCffDTffBT** possess a higher concentration of polymer chain ends, which can undergo chain-end scission. Secondly, degradation mechanisms involve molecular mobility which is inversely related to molecular weight. An increased molecular weight should reduce the amount of labile end-groups facilitating chain entanglement. Thus, the molecular mobility of the polymer, which controls the kinetics of decomposition, is reduced.

X-Ray diffraction (XRD) studies

Powder X-ray diffraction (XRD) patterns of polymers **PCDTffBT**, **PCffDTBT** and **PCffDTffBT** were obtained to investigate the molecular organisation of polymers in the solid state (Fig. 6). All polymers display peaks in the low angle region, which suggests the polymers possess some long-range translational order. An indication the polymers adopt a more crystalline structure in the solid state. The low-angle peak in the XRD pattern is frequently observed in π-conjugated polymers with long alkyl or alkoxy side-chains.[36–38] Previous literature has shown that this peak is attributed to the distance between π-conjugated backbones which are separated by the solubilising alkyl chains.[39,40]

Interestingly, **PCDTffBT** and **PCffDTffBT** display additional wide angle peaks at 2θ = 25.6°, which corresponds to a

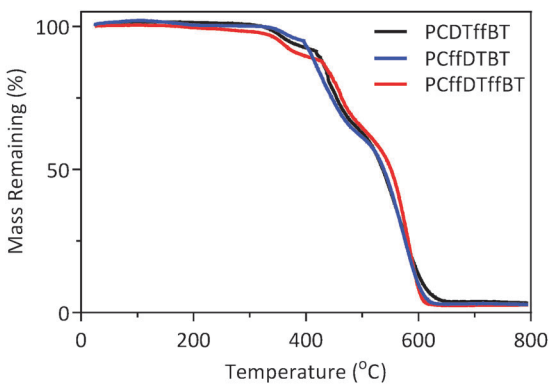

Fig. 5 Thermogravimetric analysis of **PCDTffBT**, **PCffDTBT** and **PCffDTffBT** with a heating rate of 10 °C min^{-1} under an inert nitrogen atmosphere.

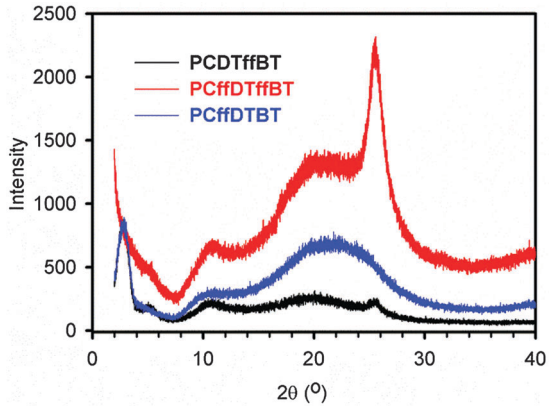

Fig. 6 Powder X-ray diffraction (XRD) patterns of **PCDTffBT**, **PCffDTBT** and **PCffDTffBT**.

π–π stacking distance of 3.48 Å. It is speculated that fluorinating the benzothiadiazole acceptor unit improves molecular ordering by promoting interactions with components on adjacent aromatics. This improves the planarity of the resulting backbone, resulting in strong interchain interactions and a more pronounced packing order. A result consistent with the reduced inhomogeneous broadening observed in the solid state spectra of **PCffDTffBT**. **PCffDTBT** does not display an additional peak in this area suggesting that fluorination of the carbazole moiety does have the same impact. Interestingly, Bo *et al.* found that **PDFCDTBT**, an analogous polymer to **PCffDTBT**, displayed a π–π stacking distance of 3.7 Å.[21] However, the carbazole moiety in **PDFCDTBT** was substituted with a significantly smaller alkyl chain (C8 linear chain *vs.* C25 branched chain). It is hypothesised that the larger alkyl chain in **PCffDTBT** disrupts the formation of π–π stacking in solid state.

Conclusions

In summary, three fluorinated carbazole-*alt*-benzothiadiazole D–π–A alternating copolymers **PCDTffBT**, **PCffDTBT** and **PCffDTffBT** were synthesised *via* Stille polymerisation using toluene as the solvent. The optical, thermal, electrochemical and structural properties of these polymers were analysed and contrasted in relation to the degree of fluorination and their fluorination pattern. The optical band gaps of **PCDTffBT**, **PCDTffBT** and **PCffDTffBT** were estimated to be 1.86, 1.82 and 1.88 eV, respectively. It is hypothesised that the lower optical band gap of **PCffDTBT** was a consequence of its higher molecular weight. The HOMO levels of **PCffDTBT** (−5.23 eV) and **PCffDTffBT** (−5.24 eV) were significantly shallower relative to that of **PCDTffBT** (−5.44 eV). It is hypothesised that the introduction of fluorine at the 3,6-positions of the carbazole unit increases its donating ability resulting in a shallower HOMO level. Thermogravimetric analysis revealed that the onset of decomposition is strongly dependent upon the molecular weight of the resulting polymer with **PCffDTBT** and **PCffDTffBT** displaying the highest and lowest decomposition temperatures, respectively. Powder X-ray diffraction revealed that all polymers possess peaks in the low angle region suggesting all polymers have some long range translational order. **PCDTffBT** and **PCffDTffBT** both displayed sharp peaks at 2θ values of 25.6°. These peaks are indicative of π–π stacking suggesting fluorination of the benzothiadiazole moiety improves the planarity of the polymer backbone, leading to a more pronounced packing order in the solid state. **PCffDTBT** did not display a shark peak at this angle.

Experimental

Experimental

All materials were purchased from commercial suppliers and used as received, unless otherwise stated. Toluene was dried and distilled over sodium under an inert argon atmosphere. Acetonitrile was dried and distilled over phosphorous pentoxide under an inert argon atmosphere, then stored over molecular sieves (3 Å).

Measurements

^{1}H and ^{13}C nuclear magnetic resonance (NMR) spectra were recorded on a Bruker AV 400 (400 MHz) using chloroform-d ($CDCl_3$) or acetone-d as the solvent. ^{1}H-NMR of the polymers were recorded on Bruker Avance III HD 500 (500 MHz) spectrometer at 100 °C using 1,2-dideutrotetrachloroethance as the solvent. Coupling constants are given in Hertz (Hz). Carbon, hydrogen, nitrogen and sulphur elemental analysis was performed on a Perkin Elmer 2400 series 11 CHNS/O analyser. Analysis of halides was undertaken using the Schöniger flask combustion method. GPC analysis was conducted on polymer solutions using 1,2,4-trichlorobenzene at 140 °C as the eluent. Polymer samples were spiked with toluene as a reference. GPC curves were obtained using a Viscotek GPCmax VE2001 GPC solvent/sample module and a Waters 410 Differential Refractometer, which was calibrated using a series of narrow polystyrene standards (Polymer Laboratories). TGA's were obtained using a Perkin Elmer TGA-1 Thermogravimetric Analyser at a scan rate of 10 °C min^{-1} under an inert nitrogen atmosphere. Powder X-ray diffraction samples were recorded on a Bruker D8 advance diffractometer with a CuKα radiation source (1.5418 Å, rated as 1.6 kW). The scanning angle was conducted over the range 2–40°. UV-visible absorption spectra were recorded using a Hitachi U-2010 Double Bean UV/Visible Spectrophotometer. Polymer solutions were made using chloroform and measured using quartz cuvettes (path length = 1 × 10^{-2} m). Thin films, used for absorption spectra were prepared by drop-casting solutions onto quartz plates using 1 mg cm^{-3} polymer solutions that were prepared with chloroform. Fluorescence spectra were recorded on a Horiba FluoroMax 4 spectrometer. Polymer solutions were made using chloroform and measured using quartz cuvettes (path length = 1 × 10^{-2} m). Thin films, were prepared by drop-casting solutions onto quartz plates using 5 mg cm^{-3} polymer solutions that were prepared with chlorobenzene. Cyclic voltammograms were recorded using a Princeton Applied Research Model 263A Potentiostat/Galvanostat.

A three electrode system was employed comprising a Pt disc, platinum wire and Ag/Ag^+ as the working electrode, counter electrode and reference electrode, respectively. Measurements were conducted in a tetrabutylammonium perchlorate acetonitrile solution (0.1 mol dm^{-3}) on polymer films that were prepared by drop casting polymer solution. Ferrocene was employed as the reference redox system; in accordance with IUPAC's recommendations.[41] The energy level of Fc/Fc^+ was assumed at −4.8 eV to vacuum. The half-wave potential of Fc/Fc^+ redox couple was found to be 0.08 V *vs.* Ag/Ag^+ reference electrode. The HOMO energy levels of polymers were estimated by equation: $E_{HOMO} = -(4.8 - E_{1/2,Fc,Fc^+} + E_{ox,onset}) = -(4.72 + E_{ox,onset})$ eV, where $E_{ox,onset}$ is the onset oxidation potential relative to the Ag/Ag^+ reference electrode. The LUMO energy levels of polymers were calculated using the equation: $E_{LUMO} = -(4.8 - E_{1/2,Fc,Fc^+} + E_{red,onset}) = -(4.72 + E_{red,onset})$ eV, where $E_{red,onset}$ is the onset reduction potential relative to the Ag/Ag^+ reference electrode.

3,6-Difluoro-2,7-dibromo-9-(pentacosan-13-yl)-9*H*-carbazole (M1). 2,7-Dibromo-3,6-difluoro-9*H*-carbazole[42] (3.0 g, 15.4 mmol) and powdered KOH (4.31 g, 41.8 mmol) were dissolved in anhydrous DMSO (100 cm^3). The mixture was heated to 40 °C and pentacosan-13-yl 4-methylbenzene (10.41 g, 19.9 mmol) in dry THF (10 cm^3) was added dropwise over 2 hours. The reaction was allowed to stir overnight. Upon completion, the reaction was poured on H_2O (300 cm^3) and the product extracted with hexane (4 × 300 cm^3). The organic fractions were combined, dried ($MgSO_4$) and the solvent removed *in vacuo*. The product was purified *via* silica gel column chromatography using hexane as the eluent to yield an off-white solid (2.43 g, 3.41 mmol, 22%). ^1H NMR (400 MHz, $CDCl_3$) δ (ppm): 7.74 (br, 3H), 7.58 (br, 1H), 4.39 (sep, J = 5.09 Hz, 1H), 2.19 (m, 2H), 1.92 (m, 2H), 1.36–1.08 (m, 38H), 0.97 (m, 2H), 0.89 (t, J = 6.94 Hz, 6H). ^{13}C NMR (250 MHz, $CDCl_3$) δ (ppm): 154.29, 151.92, 139.54, 135.89, 115.62, 113.40, 106.88, 57.35, 33.57, 31.75, 29.49, 29.37, 29.28, 29.12,, 26.73, 22.62, 14.07. ^{19}F NMR (250 MHz, $CDCl_3$) δ (ppm): −118.54, −119.06. EI-MS (m/z): $[M]^+$ calculated for $C_{37}H_{55}Br_2F_2N$, 711.2710; found, 711.2685. Anal. calculated for $C_{37}H_{55}Br_2F_2N$: C, 62.45; H, 7.71; N, 1.97; Br, 22.46; found: C, 62.08; H, 7.92; N, 1.95; Br, 23.22.

2,7-Dibromo-9-(pentacosan-13-yl)-9*H*-carbazole (M2). 2,7-Dibromo-9*H*-carbazole (5.00 g, 15.4 mmol) and powdered KOH (4.31 g, 76.9 mmol) were dissolved in anhydrous DMSO (100 cm^3). The mixture was heated to 40 °C and pentacosan-13-yl 4-methylbenzene (12.06 g, 23.08 mmol) in dry THF (20 cm^3) was added dropwise over 2 hours. The reaction was allowed to stir overnight. Upon completion, the reaction was poured on H_2O (300 cm^3) and the product extracted with hexane (4 × 300 cm^3). The organic fractions were combined, dried ($MgSO_4$) and the solvent removed *in vacuo*. The product was purified *via* silica gel column chromatography using hexane as the eluent to yield an off-white solid (4.83 g, 7.15 mmol, 46%) ^1H NMR (400 MHz, $CDCl_3$) δ (ppm): 7.92 (dd, J = 4.51 and J = 8.42 Hz, 2H), 7.73 (s, 1H), 7.57 (s, 1H), 7.35 (t, J = 7.11 Hz, 2H), 4.44 (sep, J = 2.51 Hz, 1H), 2.21 (m, 2H), 1.93 (m, 2H), 1.36–1.09 (m, 38H), 0.99 (m, 2H), 0.90 (t, J = 6.94 Hz, 6H). ^{13}C NMR (250 MHz, $CDCl_3$) δ (ppm): 122.34, 121.47, 121.22, 114.54, 112.17, 56.98, 33.51, 31.94, 29.63, 29.56, 29.49, 29.37, 29.33, 26.76, 22.72, 14.16 EI-MS (m/z): $[M]^+$ calculated for $C_{39}H_{57}Br_2NNa$, 696.2755; found, 696.2730. Anal. calculated for $C_{37}H_{57}Br_2N$: C, 65.72; H, 8.50; N, 2.07; Br, 23.65; found: C, 64.37; H, 8.39; N, 1.94; Br, 27.61.

4,7-Bis(5-(trimethylstannyl)thiophene-2-yl)benzo[*c*][1,2,5]-thiadiazole (M3). Under an inert argon atmosphere, 2,2,6,6-tetramethylpiperdine (1.46 cm^3, 8.66 mmol) was dissolved in anhydrous THF (20 cm^3). The solution was cooled to −78 °C and *n*-butyl lithium (3.46 cm^3, 8.66 mmol, 2.5 M solution in hexane) was added dropwise. The resulting solution was allowed to stir at −78 °C. The reaction was then warmed to room temperature and stirred for 10 minutes. The solution was then cooled to −78 °C and 4,7-di(thiophen-2-yl)benzo[*c*][1,2,5]-thiadiazole (1.0 g, 3.33 mmol) in THF (15 cm^3) was added dropwise. Upon complete addition, the solution was stirred at −78 °C for 1 hour. Trimethyltin chloride (8.32 cm^3, 8.33 mmol, 1.0 M solution in THF) was added dropwise at −78 °C. The reaction was warmed to room temperature and left to stir overnight. Upon completion, saturated brine was added to quench the reaction. The product was extracted with DCM (3 × 100 cm^3), washed with brine (3 × 100 cm^3), dried ($MgSO_4$) and the solvent removed *in vacuo*. The crude material was recrystallised from ethanol to afford (**M3**) as orange needle-like crystals (1.42 g, 2.27 mmol, 68%). ^1H NMR (400 MHz, $CDCl_3$) δ (ppm): 8.21 (d, J = 3.42 Hz, 2H), 7.88 (s, 2H), 7.32 (d, J = 3.67 Hz, 2H), 0.48 (s, 18H). ^{13}C NMR (400 MHz, $CDCl_3$) δ (ppm): 152.66, 154.07, 140.23, 136.26, 136.12, 135.99, 128.60, 128.40, 128.21, 125.80, −6.25. EI-MS (m/z): $[M]^+$ calculated for $C_{20}H_{24}N_2S_3Sn_2Na$, 650.9043; found, 650.9025. Anal. calculated for $C_{20}H_{24}N_2S_3Sn_2$: C, 38.37; H, 3.86; N, 4.47; S, 15.36; found: C, 38.62; H, 3.87; N, 4.50; S, 15.38.

5,6-Difluoro-4,7-bis(5-(trimethylstannyl)thiophene-2-yl)benzo-[*c*][1,2,5]thiadiazole (M4). Under an inert argon atmosphere, 2,2,6,6-tetramethylpiperdine (0.73 cm^3, 4.33 mmol) was dissolved in anhydrous THF (10 cm^3). The solution was cooled to −78 °C and *n*-butyl lithium (1.73 cm^3, 4.33 mmol, 2.5 M solution in hexane) was added dropwise. The resulting solution was allowed to stir at −78 °C. The reaction was then warmed to room temperature and stirred for 10 minutes. The solution was then cooled to −78 °C and 5,6-difluoro-4,7-di(thiophen-2-yl)benzo[*c*][1,2,5]thiadiazole (0.56 g, 1.67 mmol) in THF (15 cm^3) was added dropwise. Upon complete addition, the solution was stirred at −78 °C for 1 hour. Trimethyltin chloride (8.32 cm^3, 8.33 mmol, 1.0 M solution in THF) was added dropwise at −78 °C. The reaction was warmed to room temperature and left to stir overnight. Upon completion, saturated brine was added to quench the reaction. The product was extracted with DCM (5 × 100 cm^3), washed with brine (3 × 100 cm^3), dried ($MgSO_4$) and the solvent removed *in vacuo*. The crude material was recrystallised from ethanol to afford (**M4**) as orange powder (0.274 g, 0.414 mmol, 25%). ^1H NMR (400 MHz, $CDCl_3$) δ (ppm): 8.36 (d, J = 3.67 Hz, 2H), 7.37 (d, J = 3.42 Hz, 2H), 0.49 (s, 18H). ^{13}C NMR (250 MHz, $CDCl_3$) δ (ppm): 150.91, 150.71, 149.04, 148.33, 148.13, 142.61, 137.06, 135.52, 135.39, 135.26, 131.72, 131.55, 1.01, −6.29, −8.15. ^{19}F NMR

(250 MHz, $CDCl_3$) δ (ppm): −127.95. EI-MS (m/z): $[M]^+$ calculated for $C_{20}H_{22}F_2N_2S_3Sn_2Na_2$, 686.8855; found, 686.8879. Anal. calculated for $C_{20}H_{22}N_2S_3F_2Sn_2$: C, 36.29; H, 3.35; N, 5.74; S, 14.53; found: C, 36.84; H, 3.36; N, 4.20; S, 13.87.

Poly[*N*-9′-pentacosanyl-2,7-carbazole-*alt*-5,5-(4′,7′-di-2-thienyl-5,6-difluoro-benzo[*c*][1,2,5]-thiadiazole)] (PCDTffBT). M2 (138 mg, 0.204 mmol), **M4** (135 mg, 0.204 mmol), $Pd(OAc)_2$ (3.30 mg, 14.8 μmol) and tri(*o*-tolyl)phosphine (9.00 mg, 29.6 μmol) were added to a 100 cm^3 round bottom flask. The flask was placed under an inert atmosphere of argon using standard Schlenk line techniques. Anhydrous toluene (10 cm^3) was added, the system degassed and heated to 90 °C for 48 hours. Upon completion, the reaction was cooled to room temperature and 2-(tributylstannyl)thiophene (0.30 cm^3, 0.945 mmol) was added. The mixture was degassed and heated at 90 °C for 1.5 hours. The mixture was cooled to room temperature and 2-bromothiophene (0.30 cm^3, 3.10 mmol) was added, the system degassed and heated at 90 °C for 2 hours. The reaction was cooled to room temperature and poured into methanol and left to stir overnight. The mixture was filtered through a membrane and the solids were cleaned using Soxhlet extraction with solvents in the order; methanol, acetone, hexane and toluene. The toluene fraction was concentrated *in vacuo* and precipitated in methanol. The resulting mixture was stirred overnight and the polymers collect *via* filtration as a deep purple powder (107 mg, 62%) GPC toluene fraction, M_n = 7700 g mol^{-1}, M_w = 11 900 g mol^{-1}, PDI = 1.55. ^{1}H NMR (500 MHz, $C_2D_2Cl_4$, 100 °C) (δ_H/ppm) 8.37 (m, 2H), 8.11 (m, 2H), 7.61 (m, 2H), 7.56 (m, 2H), 4.68 (br, 1H), 2.39 (br, 2H), 2.09 (br, 2H) 1.39–1.04 (br, 40), 0.84 (m, 6H). Anal. calculated for $C_{51}H_{61}F_2N_3S_3$: C, 72.03; H, 7.23; N, 4.94; S, 11.31; found: C, 71.16; H, 7.33; N, 4.72; S, 10.47.

Poly[*N*-9′-pentacosanyl-3,6-difluoro-2,7-carbazole-*alt*-5,5-(4′,7′-di-2-thienyl-benzo[*c*][1,2,5]-thiadiazole)] (PCffDTBT). PCffDTBT was synthesized according to the procedure outlined in **PCDTffBT**. **M1** (145 mg, 0.204 mmol), **M3** (128 mg, 0.204 mmol), $Pd(OAc)_2$ (3.30 mg, 14.8 μmol) and tri(*o*-tolyl)phosphine (9.00 mg, 29.6 μmol) were added to a 100 cm^3 round bottom flask. The flask was placed under an inert atmosphere of argon using standard Schlenk line techniques. Anhydrous toluene (10 cm^3) was added, the system degassed and heated to 90 °C for 48 hours. The polymer was obtained as a deep purple solid (112 mg, 65%) GPC toluene fraction, M_n = 11 400 g mol^{-1}, M_w = 20 600 g mol^{-1}, PDI = 1.81. ^{1}H NMR (500 MHz, $C_2D_2Cl_4$, 100 °C) (δ_H/ppm) 8.21 (br, 2H), 7.95 (br, 2H), 7.72 (4H, br), 7.63 (br, 2H), 4.59 (br, 2H), 2.35 (br, 2H), 2.07 (br, 2H), 1.39–1.12 (br, 40H), 0.84 (m, 6H). Anal. calculated for $C_{51}H_{61}F_2N_3S_3$: C, 72.03; H, 7.23; N, 4.94; S, 11.31; found: C, 70.03; H, 6.23; N, 5.36; S, 12.35.

Poly[*N*-9′-pentacosanyl-3,6-difluoro-2,7-carbazole-*alt*-5,5-(4′,7′-di-2-thienyl-5,6-difluoro-benzo[*c*][1,2,5]-thiadiazole)] (PCffDTffBT). PCffDTffBT was synthesized according to the procedure outlined in **PCDTffBT**. **M1** (145 mg, 0.204 mmol), **M4** (135 mg, 0.204 mmol), $Pd(OAc)_2$ (3.30 mg, 14.8 μmol) and tri(*o*-tolyl)phosphine (9.00 mg, 29.6 μmol) were added to a 100 cm^3 round bottom flask. The flask was placed under an inert atmosphere of argon using standard Schlenk line techniques. Anhydrous toluene (10 cm^3) was added, the system degassed and heated to 90 °C for 48 hours. The polymer was obtained as a deep purple solid (40.8 mg, 23%) GPC toluene fraction, M_n = 6100 g mol^{-1}, M_w = 8900 g mol^{-1}, PDI = 1.46. ^{1}H NMR (500 MHz, $C_2D_2Cl_4$, 100 °C) (δ_H/ppm) 8.38 (m, 2H), 7.82–7.59 (br, 6H), 4.60 (br, 1H), 2.34 (br, 2H), 2.07 (br, 2H), 1.39–1.03 (br, 40H), 0.83 (m, 6H). Anal. calculated for $C_{51}H_{59}F_4N_3S_3$: C, 69.12; H, 6.71; N, 4.74; S, 10.85. Found: C, 63.88; H, 5.27; N, 5.26; S, 13.14.

Acknowledgements

We would like to thank the University of Sheffield for the award of a scholarship (L. C.) and EPSRC for financial support of this work *via* research grant EP/I028641/1.

References

1 Y. Cheng, S. Yang and C. Hsu, *Chem. Rev.*, 2009, **109**, 5868–5923.
2 V. N. Bliznyuk, S. A. Carter, J. C. Scott, G. Kla, R. D. Miller and D. C. Miller, *Macromolecules*, 1999, **32**, 361–369.
3 W. Yue, Y. Zhao, S. Shao, H. Tian, Z. Xie and F. Wang, *J. Mater. Chem.*, 2009, **19**, 2199–2206.
4 A. Iraqi and I. Wataru, *Chem. Mater.*, 2004, **42**, 442–448.
5 K. Zhang, Y. Tao, C. Yang, H. You, Y. Zou, J. Qin and D. Ma, *Chem. Mater.*, 2008, **20**, 7324–7331.
6 N. Agarwal, P. K. Nayak, F. Ali, M. P. Patankar, K. L. Narasimhan and N. Periasamy, *Synth. Met.*, 2011, **161**, 466–473.
7 P. T. Boudreault, S. Wakim, L. Tang, Y. Tao, Z. Bao and M. Leclerc, *J. Mater. Chem.*, 2009, **19**, 2921–2928.
8 A. Van Dijken, J. J. A. M. Bastiaansen, N. M. M. Kiggen, B. M. W. Langeveld, C. Rothe, A. Monkman, I. Bach, P. Stössel and K. Brunner, *J. Am. Chem. Soc.*, 2004, **126**, 7718–7727.
9 B. N. Drolet, J. F. Morin, N. Leclerc, S. Wakim, Y. Tao and M. Leclerc, *Adv. Funct. Mater.*, 2005, **15**, 1671–1682.
10 Y. Sun, J. H. Seo, C. J. Takacs, J. Seifter and A. J. Heeger, *Adv. Mater.*, 2011, **23**, 1679–1683.
11 H. Yi, S. Al-Faifi, A. Iraqi, D. C. Watters, J. Kingsley and D. G. Lidzey, *J. Mater. Chem.*, 2011, **21**, 13649–13656.
12 Z. He, C. Zhong, X. Huang, W. Wong, H. Wu, L. Chen, S. Su and Y. Cao, *Adv. Mater.*, 2011, **23**, 4636–4643.
13 C. Gu, Y. Chen, Z. Zhang, S. Xue, S. Sun, C. Zhong, H. Zhang, Y. Lv, F. Li, F. Huang and Y. Ma, *Adv. Energy Mater.*, 2014, **4**, 1–5.
14 Y. Liu, J. Zhao, Z. Li, C. Mu, W. Ma, H. Hu, K. Jiang, H. Lin, H. Ade and H. Yan, *Nat. Commun.*, 2014, **5**, 1–8.
15 S. Beaupré and M. Leclerc, *J. Mater. Chem. A*, 2013, **1**, 11097–11105.
16 J. W. Kingsley, P. P. Marchisio, H. Yi, A. Iraqi, C. J. Kinane, S. Langridge, R. L. Thompson, A. J. Cadby, A. J. Pearson, D. G. Lidzey, R. A. L. Jones and A. J. Parnell, *Sci. Rep.*, 2014, 5286.
17 A. Casey, Y. Han, Z. Fei, A. J. P. White, T. D. Anthopoulos and M. Heeney, *J. Mater. Chem. C*, 2015, **3**, 265–275.

18 J. W. Jo, J. W. Jung, E. H. Jung, H. Ahn, T. J. Shin and W. H. Jo, *Energy Environ. Sci.*, 2015, **8**, 2427–2434.
19 G. Li, C. Kang, X. Gong, J. Zhang, W. Li, C. Li, H. Dong, W. Hu and Z. Bo, *J. Mater. Chem. C*, 2014, **2**, 5116–5123.
20 N. Wang, Z. Chen, W. Wei and Z. Jiang, *J. Am. Chem. Soc.*, 2013, **135**, 17060–17068.
21 C. Du, W. Li, Y. Duan, C. Li, H. Dong, J. Zhu, W. Hu and Z. Bo, *Polym. Chem.*, 2013, **4**, 2773–2782.
22 J. Kim, M. H. Yun, G. Kim, J. Lee, S. M. Lee, S. Ko, Y. Kim, G. K. Dutta, M. Moon, S. Y. Park, D. S. Kim, J. Y. Kim and C. Yang, *ACS Appl. Mater. Interfaces*, 2014, **6**, 7523–7534.
23 H. Wei, Y. Chao, C. Kang, C. Li, H. Lu, X. Gong, H. Dong, W. Hu, C. Hsu and Z. Bo, *Macromol. Rapid Commun.*, 2015, **36**, 84–89.
24 T. Umeyama, Y. Watanabe, E. Douvogianni and H. Imahori, *J. Phys. Chem. C*, 2013, **117**, 21148–21157.
25 B. N. Blouin, A. Michaud and M. Leclerc, *Adv. Mater.*, 2007, **19**, 2295–2300.
26 L. Cartwright, A. Iraqi, Y. Zhang, T. Wang and D. G. Lidzey, *RSC Adv.*, 2015, **5**, 46386–46394.
27 Y. Zhang, S. C. Chien, K. S. Chen, H. L. Yip, Y. Sun, J. A. Davies, F. C. Chen and A. K. Y. Jen, *Chem. Commun.*, 2011, **47**, 11026–11028.
28 Z. Li, J. Lu, S.-C. Tse, J. Zhou, X. Du, Y. Tao and J. Ding, *J. Mater. Chem.*, 2011, **21**, 3226–3233.
29 S. Albrecht, S. Janietz, W. Schindler, J. Frisch, J. Kurpiers, J. Kniepert, S. Inal, P. Pingel, K. Fostiropoulos, N. Koch and D. Neher, *J. Am. Chem. Soc.*, 2012, **134**, 14932–14944.
30 H. Zhou, L. Yang, A. C. Stuart, S. C. Price, S. Liu and W. You, *Angew. Chem., Int. Ed.*, 2011, **50**, 2995–2998.
31 A. Iyer, J. Bjorgaard, T. Anderson and M. E. Köse, *Macromolecules*, 2012, **45**, 6380–6389.
32 T. X. Carroll, T. D. Thomas, H. Bergersen, K. J. Børve and L. J. Sæthre, *J. Org. Chem.*, 2006, **71**, 1961–1968.
33 J. Rosenthal and D. I. Schuster, *J. Chem. Educ.*, 2003, **80**, 679–690.
34 R. Yamdagni and P. Kebarle, *J. Am. Chem. Soc.*, 1976, **98**, 1320–1324.
35 Z. B. Maksić, B. Kovačević and D. Kovaček, *J. Phys. Chem. A*, 1997, **101**, 7446–7453.
36 H. Fang, J. W. Lin, I. H. Chiang, C. W. Chu, K. H. Wei and H. Lin, *J. Polym. Sci., Part A: Polym. Chem.*, 2012, **50**, 5011–5022.
37 H. Fukumoto and T. Yamamoto, *J. Polym. Sci., Part A: Polym. Chem.*, 2008, **5**, 2975–2982.
38 H. Li, P. Tang, Y. Zhao, S. X. Liu, Y. Aeschi, L. Deng, J. Braun, B. Zhao, Y. Liu, S. Tan, W. Meier and S. Decurtins, *J. Polym. Sci., Part A: Polym. Chem.*, 2012, **50**, 2935–2943.
39 T. Yamamoto, Q. Fang and T. Morikita, *Macromolecules*, 2003, **36**, 4262–4267.
40 T. Yamamoto, *Macromol. Rapid Commun.*, 2002, **23**, 583–606.
41 G. Gritzner, *Pure Appl. Chem.*, 1990, **62**, 1839–1858.
42 H. Kun, H. Yi, R. G. Johnson and A. Iraqi, *Polym. Adv. Technol.*, 2008, **19**, 299–307.

